Astron. Astrophys. 335, 973–978 (1998)

ASTRONOMY AND ASTROPHYSICS

Magnetic field models for A and B stars

V. The magnetic field and photometric variation of 84 Ursae Majoris

G.A. Wade[1], **G.M. Hill**[2,4,5], **S.J. Adelman**[3], **N. Manset**[4], **and P. Bastien**[4]

[1] Physics & Astronomy Department, The University of Western Ontario, London, Ontario, N6A 3K7, Canada
[2] Hertzberg Institute of Astrophysics, Dominion Astrophysical Observatory, 501 West Saanich Road, Victoria, B.C., V8X 4M6, Canada
[3] Department of Physics, The Citadel, 171 Moultrie Street, Charlston, SC 29409, USA
[4] Département de Physique, Université de Montréal, C.P. 6128, Succ. Centre-Ville, Montréal, PQ, H3C 3J7, Canada,
[5] McDonald Observatory, University of Texas at Austin, P.O. Box 1337, Fort Davis, TX 79734, USA

Received 29 December 1997 / Accepted 14 April 1998

Abstract. We present new longitudinal magnetic field and Strömgren photometric measurements[1] of the Bp star 84 UMa. From these data we determine a new rotational period $P_{rot} = 1.^d38576 \pm 0.^d00080$, which is inconsistent with previously published values.

The magnetic measurements indicate the presence of a weak, dominantly dipolar magnetic field in the photosphere of 84 UMa. We employ a new value of the rotational axis inclination in conjunction with the magnetic data in order to constrain the magnetic field geometry. We derive the following dipole oblique rotator parameters: $i = 59^{+17\mathrm{o}}_{-9}$, $\beta = 48^{+17\mathrm{o}}_{-29}$, and $B_\mathrm{d} = 1620^{+1270}_{-30}$ G.

A precise value of the radius (which we calculate in conjunction with the inclination using the Hipparcos parallax) allows us to locate 84 UMa on the radius-effective temperature plane. Using theoretical evolutionary tracks (Schaller et al. 1992), we obtain values for the mass, age and surface gravity. These results place 84 UMa quite close to the ZAMS, a result inconsistent with the suggestion by Hubrig & Mathys (1994) that the magnetic Ap stars may be near the end of their main sequence life.

Key words: stars: chemically peculiar – stars: individual: 84 UMa – stars: magnetic fields – polarization

1. Introduction

The inhomogeneous distributions of surface chemical abundance observed in the Ap and Bp stars are thought to result from a complex interplay between gravitational and radiative diffusion, mass loss, turbulence and circulation processes in their atmospheres (Michaud & Proffitt 1993). By determining the magnetic field geometries and surface chemical abundance distributions of a representative sample of these objects, important new contraints can be placed upon the manner in which and degree to which these processes interact with the magnetic field. This paper represents the fifth in a series (Wade et al. 1996a, Wade et al. 1996b, Wade et al. 1997a, Wade et al. 1997b) aimed at constructing such models of the magnetic fields of A and B stars.

84 Ursae Majoris (=HD 120198=HR 5187) is a moderately broad-lined B9p EuCr star (Hoffleit 1982) which exhibits modest spectrum variability (Rice & Wehlau 1994, hereafter R&W). The rotational period has been reported by Burke & Barr (1981) to be $1.^d37996 \pm 0.^d00008$ from UBV photometry. However, R&W find a slightly better period solution by removing 1 presumably spurious point from the photometry, and adopt $1.^d380682$ as the rotational period. Using the latter period, R&W obtained Doppler images of the Fe and Cr abundance distributions of 84 UMa. The resultant maps are similar to one another, and quite complex.

2. Observations

2.1. Longitudinal magnetic field

Longitudinal magnetic field (B_l) measurements were obtained at the University of Western Ontario (UWO) Elginfield Observatory, and at the Observatoire du Mont Mégantic (OMM), between JD 2449823 and 2450659. As well, we include three measurements obtained by Borra & Landstreet (1980) at UWO.

UWO observations were obtained using the UWO photoelectric polarimeter as a Balmer line Zeeman analyser at the UWO 1.2-metre telescope. This instrument measures the fractional circular polarisation in the wings of Hβ at ± 5.0 Å from line centre. The quantity thus measured is linearly related to the line-of-sight component of any magnetic field present in the line-forming region, suitably weighted and integrated over the stellar disk. For these observations, a mean conversion factor $\gamma = 13050$ G per percent circular polarisation was found from Hβ line scans. A more detailed description of the instrument and observing technique is given by Landstreet (1980).

The OMM photoelectric polarimeter (Manset & Bastien 1995) is a virtually identical instrument, which employs similar

Send offprint requests to: G.A. Wade, (gwade@astro.uwo.ca)

[1] Table 2 is available only in electronic form at the CDS via anonymous ftp 130.79.128.5

Table 1. Journal of longitudinal magnetic field observations of 84 UMa acquired at the UWO Elginfield Observatory (UWO) and Observatoire du Mont Mégantic (OMM). The three observations obtained by Borra & Landstreet (1980) (between JD 2442770 and 2443650) are also included. Phases are calculated from the ephemeris cited in the text and σ_B is the 1 standard deviation uncertainty derived from Poisson statistics.

JD (mid-exposure)	Phase	$B_l \pm \sigma_B$ (G)	Observatory
2442770.058	0.347	-380 ± 265	UWO
2443648.713	0.408	-125 ± 305	UWO
2443649.791	0.186	240 ± 265	UWO
2449823.655	0.405	-110 ± 150	UWO
2450046.906	0.508	-340 ± 165	OMM
2450051.894	0.108	225 ± 150	OMM
2450081.898	0.759	225 ± 170	UWO
2450138.785	0.811	670 ± 140	UWO
2450181.794	0.847	320 ± 170	UWO
2450184.743	0.975	260 ± 170	UWO
2450198.633	0.998	350 ± 140	UWO
2450266.667	0.094	175 ± 140	UWO
2450269.647	0.244	210 ± 130	UWO
2450540.786	0.905	400 ± 120	UWO
2450548.672	0.596	140 ± 140	UWO
2450564.636	0.116	360 ± 130	UWO
2450568.720	0.063	290 ± 210	UWO
2450576.647	0.783	440 ± 130	UWO
2450641.756	0.767	365 ± 200	UWO
2450645.696	0.611	-130 ± 130	UWO
2450659.670	0.694	390 ± 130	UWO

narrow-band filters. It was employed in an analogous manner on the OMM 1.6-metre telescope.

The journal of longitudinal magnetic field observations is shown in Table 1.

2.2. Strömgren photometry

276 differential $uvby$ photometric observations of 84 UMa (69 observations in each filter) were obtained during the sixth year of operation (Sept. 1995 - July 1996) of the 0.75-m Four College Automated Photoelectric Telescope (FCAPT; Dukes et al. 1992) when it was on Mount Hopkins, Arizona. After the dark count was measured, the telescope, in each filter, obtained sky-ch-c-v-c-v-c-v-c-ch-sky measurements where ch is a reading of the check star HR 5169 (= HD 119765, spectral type A1 V), c that of the comparison star 86 UMa (= HR 5238 = HD 121409, spectral type A0 V), and v that of 84 UMa. The data were converted to instrumental magnitudes using a spread sheet reduction program which employs mean seasonal extinction coefficients. Usually only one set of $uvby$ measurements were made of 84 UMa and its comparison and check stars each clear night. The Strömgren photometry is presented in Table 2, which is available only in electronic form at the CDS via anonymous ftp 130.79.128.5.

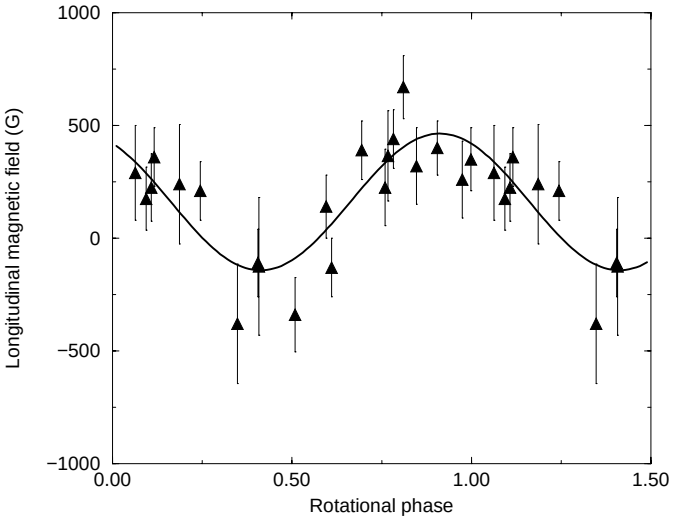

Fig. 1. Observed and computed longitudinal magnetic field variation of 84 UMa, phased according to the ephemeris described in the text. The solid curve is the variation produced by the best-fit magnetic field geometry, described in Sect. 5.1.

2.3. Hipparcos photometry

125 photometric measurements of 84 UMa were obtained in the context of the Hipparcos mission, in the Hipparcos photometric system described in Volume 1 of The Hipparcos and Tycho Catalogues (ESA 1997). The photometry is available in Volume 17 of the Hipparcos Catalogue, CD-ROM no. 3 (ESA 1997). The standard errors of the Hipparcos magnitudes of the Strömgren photometry check and comparison stars (HR 5169 and 86 UMa, respectively) are $0\overset{\mathrm{m}}{.}0006$ and $0\overset{\mathrm{m}}{.}0005$, respectively. This confirms the Strömgren photometric result that they are sufficiently non-variable to be used as comparison stars for differential photometry.

3. Period analysis

Each of the three datasets (longitudinal field, Strömgren photometry and Hipparcos photometry) was individually searched for all independent periods between 0.1 and 100 days using a Lomb-Scargle search algorithm (Press & Rybicki 1989). The only period consistent with all of the data is $1\overset{d}{.}38576 \pm 0\overset{d}{.}00080$. Most notably, none of these datasets are consistent with the $1\overset{d}{.}37996 \pm 0\overset{d}{.}00008$ reported by Burke & Barr (1981) or the $1\overset{d}{.}380682$ period employed by R&W. Both of these earlier periods rely on a very limited number of low-SNR UBV photometric observations obtained by multiple authors (34 observations by Burke & Barr 1981 and 15 observations by Winzer 1974). As a matter of fact, the periods reported by Burke & Barr (1981) and R&W are consistent within quoted uncertainties with the 1/y alias $P_{1/y} = 1\overset{d}{.}38052$ of the period implied by our data. It would therefore appear that noise and the statistics of small numbers conspired to produce misleading periodograms in these earlier studies.

When all three datasets are phased according to the new $1\overset{d}{.}38576$ period, the variations are harmonic with min-

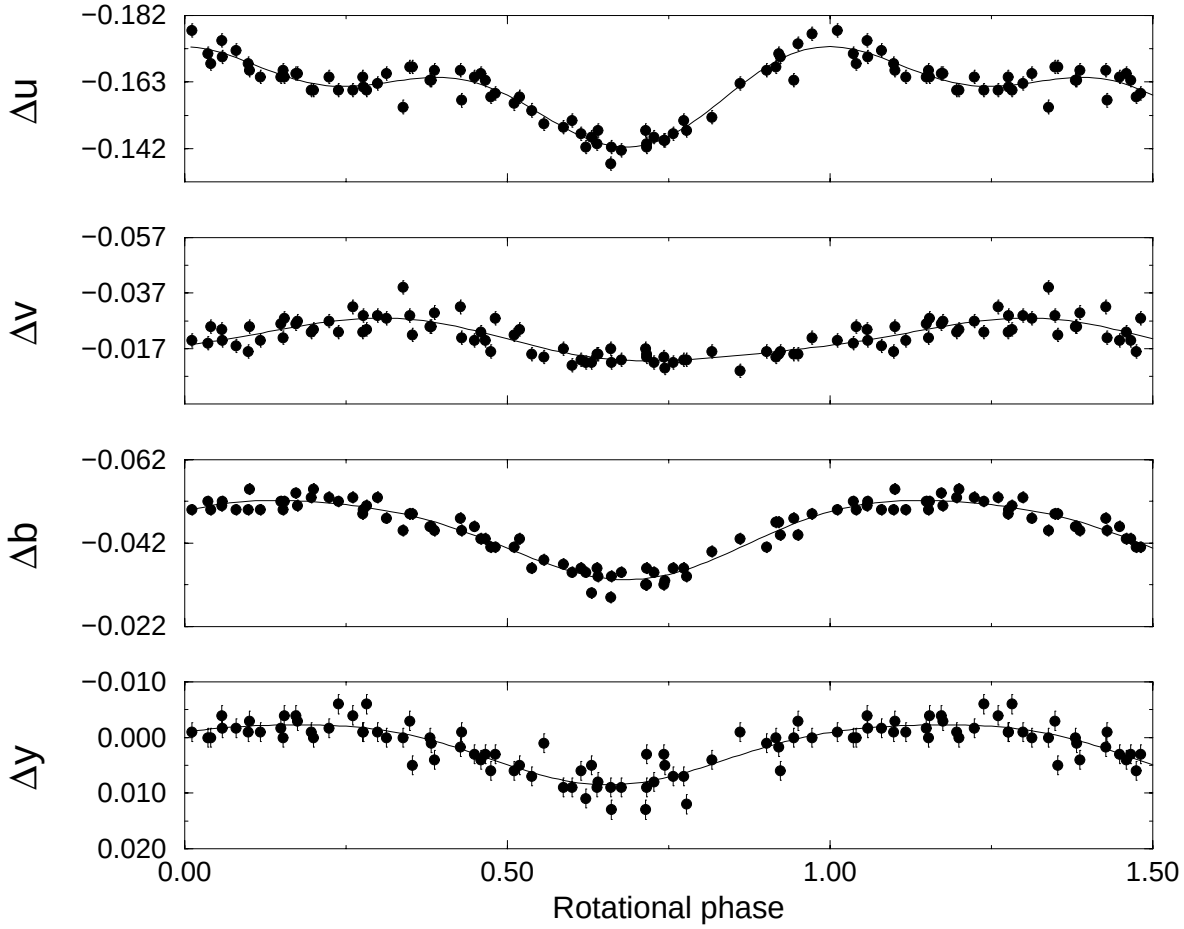

Fig. 2. Strömgren photometry of 84 UMa, phased according to the ephemeris described in the text. The solid curves are second-order least-squares Fourier fits.

imal scatter. Adopting the epoch of u-band maximum light JD 2449824.480 ± 0.03 as phase 0.0, we have phased all of the data according to the ephemeris:

$$\mathrm{JD} = 2449824.480 \pm 1.^d38576 \cdot \mathrm{E}. \quad (1)$$

The phased magnetic data are presented in Table 1, while the phased Strömgren photometry is listed in Table 2, available only in electronic form at the CDS. As well, the phased magnetic observations are shown in Fig. 1. The phased Strömgren photometry, shown in Fig. 2, shows small differences among the light curve shapes. These differences reflect that these values represent an integration over the stellar surface, which displays a complex distribution of elemental abundances (R&W). We do not display the Hipparcos photometry, since it only serves to support the results from the Strömgren photometry and magnetic field measurements (and provides no additional constraint on the period).

4. Magnetic field variation

The reduced χ^2 of a first order sine fit to the phased magnetic data is 1.0. In order to determine the significance of the detection of field variability, we can compare this to the reduced χ^2 of 4.9 for a straight line fit through $B_l = 0$ (the zero-field hypothesis). If we assume that $B_l = 0$ is a correct representation of the longitudinal field variation, the probability of obtaining a reduced χ^2 of 4.9 from 21 measurements is considerably less than 0.1%. The detection of longitudinal field variability is therefore undoubtably real, and we can characterise it using the parameters which define the 1^{st}-order sine fit:

$$B_l = B_0 + B_1 \ \sin \ 2\pi(\phi - \phi_0), \quad (2)$$

with $B_0 = 161 \pm 24$ G, $B_1 = 303 \pm 48$ G, and $\phi_0 = 0.66 \pm 0.1$. The longitudinal magnetic field of 84 UMa is clearly quite weak, with a peak-to-peak amplitude of about 600 G. This can be contrasted with the B_l variation of peculiar stars with very strong fields, such as HD 119419 or HD 126515, for which the peak-to-peak amplitude of the longitudinal field variation is about 6000 G (Mathys 1991). However, such objects appear to be relatively rare, and represent only the high-field tail of the distribution of magnetic A and B stars. Stars such as 84 UMa, with longitudinal field variability of order 100 G, are far more representative of the magnetic A and B stars as a population (Bohlender & Landstreet 1990). However, as accurate measurement of the fields of such objects is relatively difficult, they are poorly represented in the literature.

5. Surface structure

5.1. Magnetic field geometry

Doppler abundance maps of the surface Fe and Cr distributions of 84 UMa were reported by R&W. In order to construct these maps, it was necessary that they adopt a value of i, the inclination of the stellar rotational axis to the line-of-sight. R&W determined $i = 45^{\rm o}$ by assuming a radius for 84 UMa of $2.5 R_{\odot}$. With the availability of Hipparcos trigonometric parallax measurements, we expect to be able to improve upon the accuracy of their radius estimate, and therefore upon the accuracy of the inferred inclination.

The trigonometric parallax of 84 UMa is 11.58 ± 0.60 mas (ESA 1997). If we employ this value in conjunction with the angular diameter, we can calculate the stellar radius.

Stepien and Dominiczak (1989) calculated the angular diameter $\theta = 0.21$ mas of 84 UMa by comparing the observed and computed fluxes. Given the strong sensitivity of the inferred angular diameter to the assumed effective temperature, we have re-evaluated the angular diameter from the fluxes reported by these authors, employing effective temperatures from several sources (Adelman 1985, Hauck & North 1982/1993, Stepien & Dominiczak 1989). This analysis yields $T_{eff} = 9780 \pm 350$ K, giving $\theta = 0.223 \pm 0.02$ mas. From this we obtain the stellar radius $R = 2.07 \pm 0.2\ R_{\odot}$. If we furthermore employ the value of $v_e \sin i = 65 \pm 1.5$ km s^{-1} (R&W, Rice 1998), we can invoke rigid rotation to determine the inclination $i = 59^{+17{\rm o}}_{-9}$.

With our inferred value of the inclination angle, we have sufficient information with which to fit the observed longitudinal field variation using the simplest magnetic field geometry consistent with a sinusoidal variation: an oblique magnetic dipole. The oblique magnetic dipole is a 3-parameter model, and since only two formal constraints are provided by the longitudinal field variation (the two extrema), such a field geometry cannot be uniquely determined using longitudinal field measurements alone. However, we have determined i based on arguments independent of the magnetic data. The two longitudinal field constraints therefore determine the two remaining parameters in the model, the obliquity β of the magnetic field axis relative to the rotational axis, and the polar strength of the magnetic dipole $B_{\rm d}$. The obliquity angle β is calculated via the expression:

$$\tan\beta = \Big(\frac{1-r}{1+r}\Big)\cot i, \qquad (3)$$

where the parameter r is the ratio of the longitudinal magnetic extrema (Preston 1967). In the case of 84 UMa, $r = -0.30 \pm 0.13$, and we find $\beta = 48^{+17{\rm o}}_{-29}$.

The polar field strength $B_{\rm d}$ can be computed using the expression:

$$B_{\rm d} = 20 \cdot B_l^{max}\Big(\frac{3-u}{15+u}\Big)\Big(\cos\beta\cos i + \sin\beta\sin i\Big)^{-1}, \qquad (4)$$

as adapted from Preston (1967), where B_l^{max} is the value of the longitudinal field at maximum. We have assumed a value of the limb-darkening coefficient $u = 0.4$, which has been estimated from a fit to the limb darkening profile synthesized using a ($T_{\rm eff} = 10000$ K, $\log g = 4.0$) ATLAS9 model atmosphere (Kurucz 1992). We obtain $B_{\rm d} = 1620^{+1270}_{-30}$ G, where the weak constraint on the upper limit results from the divergence of $B_{\rm d}$ for $i \to 90^{\rm o}$.

These results are inconsistent with the suggestion by R&W that the magnetic field of 84 UMa has a complex global structure (which they suggest might account for the complexity of their abundance maps). While some contribution from higher-order multipoles is both possible and likely, the modeling described above shows that the field is *predominantly* dipolar, and in this sense similar to the fields of the majority of magnetic A and B stars.

The longitudinal field variation computed from the best-fit model described above is compared with the phased magnetic observations in Fig. 1.

5.2. Chemical abundance distributions

By comparing the magnetic field geometry and surface chemical abundance distributions we have the potential to confront the predictions of chemical diffusion models with observations. However, our model of the magnetic field geometry of 84 UMa is not strongly constrained. In particular, the large uncertainty associated with β means that the location in latitude of either magnetic pole is uncertain by about $45^{\rm o}$. Comparing detailed Doppler images with such an uncertain magnetic geometry is not very useful.

In addition, there are two other factors which complicate the interpretation of the abundance maps. Severe blending is encountered in the line profiles of this star (Rice 1998), and suggests that the detailed validity of the abundance maps may be compromised. As well, the unusually large (4 km s^{-1}) microturbulent velocity employed by R&W will almost certainly have an important effect on the abundance scale of their maps, which may well be underestimated by as much as 1.5 dex (Wade et al. 1997c).

Clearly, we are limited in the quantity and quality of information we can obtain about 84 UMa with the current data. We would like to point out that circular polarisation échelle spectra (obtainable at a facility such as Pic du Midi Observatory, using the MuSiCoS spectropolarimeter) could be employed in conjunction with Least-Squares Deconvolution (Donati et al. 1997, Wade et al. 1998) in order to extract unblended mean spectral line profiles as well as high signal-to-noise ratio mean circular polarisation profiles for 84 UMa. These profiles could then be used to generate Doppler abundance maps free from any ambiguity due to line blending, as well as a magnetic field model with well-constrained ($\pm 10^{\rm o}$) i and β angles. This would represent an important improvement over the current results.

6. Evolutionary state

The precise radius derived in Sect. 5 can be used in conjunction with the effective temperature in order to determine the location of 84 UMa in the radius-effective temperature ($\log\big(\frac{R}{R_{\odot}}\big) - \log T_{\rm eff}$) plane. Using model evolutionary calcula-

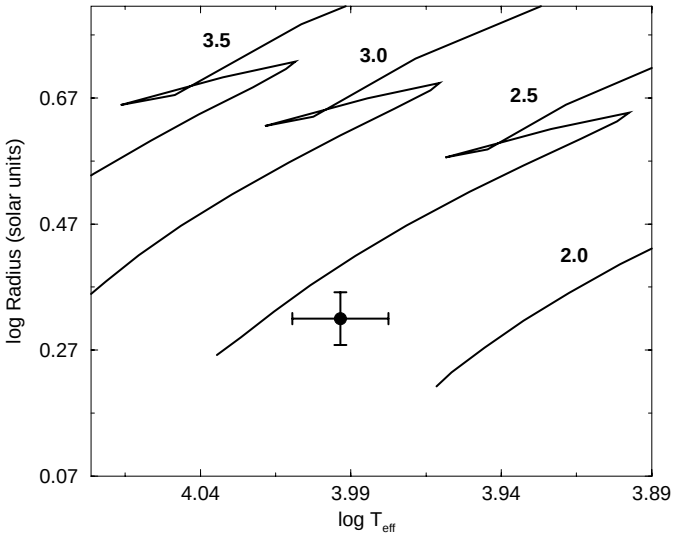

Fig. 3. Position of 84 UMa in the $\log\left(\frac{R}{R_\odot}\right) - \log T_{\rm eff}$ plane. Evolutionary tracks (from Schaller et al. 1992) are labeled in solar masses.

Table 3. Summary of physical data for 84 UMa.

d	86.4 ± 4.5 pc
R	$2.07 \pm 0.2\ R_\odot$
M	$2.35 \pm 0.15\ M_\odot$
Age	$(2.5 \pm 1.5) \times 10^8$ y
v_e	76 ± 7 km s^{-1}
P_{rot}	$1.^d38576 \pm 0.^d00080$
T_{eff}	9780 ± 350 K
$\log g$	4.18 ± 0.1
i	$i = 59^{+17o}_{-9}$
β	$\beta = 48^{+17o}_{-29}$
$B_{\rm d}$	$B_{\rm d} = 1620^{+1270}_{-30}$ G

tions, the mass and age can be inferred (e.g. Wade 1997). In Fig. 3 we show the $\log\left(\frac{R}{R_\odot}\right) - \log T_{\rm eff}$ position of 84 UMa, as well as the transformed theoretical evolutionary tracks for solar metallicity calculated by Schaller et al. (1992). From Fig. 3 we find the mass $M = 2.35 \pm 0.15\ M_\odot$ and age $A = (2.5 \pm 1.5) \times 10^8$ y of 84 UMa. From M and R we can furthermore determine the surface gravity $\log g = 4.18 \pm 0.1$.

These data place 84 UMa close to the ZAMS, a result inconsistent with the suggestion by Hubrig & Mathys (1994) that the magnetic Ap stars may be near the end of their main sequence life.

A summary of our evolutionary data for 84 UMa, as well as the rotational and magnetic data obtained in Sect. 3 and Sect. 5.1, is provided in Table 3.

7. Summary

From an analysis of new longitudinal magnetic field and Strömgren photometric measurements of the Bp star 84 UMa, we infer a rotational period of $1.^d38576 \pm 0.^d00080$. Our observations are inconsistent with the periods reported previously by Burke & Barr (1981) and Rice & Wehlau (1994), and we conclude that these periods represent the 1/y alias of our adopted period.

By considering the sinusoidal longitudinal field variation and our computed constraint on the rotational axis inclination $i = 59^{+17o}_{-9}$, we have constrained the magnetic field geometry of 84 UMa and find $\beta = 48^{+17o}_{-29}$ and $B_{\rm d} = 1620^{+1270}_{-30}$ G for the magnetic obliquity and dipole polar strength, respectively. These results are inconsistent with the suggestion by Rice & Wehlau (1994) that the magnetic field of 84 UMa has a complex global structure.

Using a precise new value of the radius (computed using the Hipparcos parallax), we have inferred the mass, age and surface gravity of 84 UMa using the theoretical evolutionary tracks of Schaller et al. (1992). These results place 84 UMa quite close to the ZAMS, a result inconsistent with the suggestion by Hubrig & Mathys (1994) that the magnetic Ap stars may be near the end of their main sequence life.

Acknowledgements. This work has been supported in part by the Natural Sciences and Engineering Research Council of Canada, the governments of Ontario and Québec and a grant from the Theodore Dunham, Jr. Fund for Astrophysical Research.

SJA's research with FCAPT telescope has been supported in part by NSF grant AST-9528506 to The Citadel and in part by grants from The Citadel Development Foundation. SJA appreciates the continuing efforts of L.J. Boyd and R.J. Dukes, Jr. to keep the FCAPT operating properly.

As well, we have made use of the Simbad database, operated at CDS, Strasbourg, France.

We would like the thank the referee T. Lanz for suggestions which improved the overall quality of this paper. Thanks also to R. Kuschnig for helpful comments regarding Doppler images.

References

Adelman S.J., 1985, PASP 97, 970
Bohlender D.A. & Landstreet J.D., 1990, MNRAS 247, 606
Borra E.F. & Landstreet J.D., 1980, ApJS 42, 421
Burke E.W. & Barr T.H., 1981, PASP 93, 344
Donati J.-F., Semel M., Carter B.D., Rees D.E., Cameron A.C., 1997, MNRAS 291, 658
Dukes, R. J., Jr., Adelman, S. J., Pyper, D. M., McCook, G. P., Guinan, E. F., 1992, in *Automated Telescopes for Photometry and Imaging*, ASP Conference Series, Vol 28, p. 21
ESA, 1997, ESA SP-1200, The Hipparcos and Tycho Catalogues, Vol. 1
Hauck B. & North P., 1982, A&A 114, 23
Hauck B. & North P., 1993, A&A 269, 403
Hoffleit D., 1982, *The Bright Star Catalogue, 4th revised ed.*, New Haven, Yale University Observatory
Kurucz R.L., 1992, in *The Stellar Populations of Galaxies*, IAU Symposium 149, p. 225
Kuschnig R., 1998, private communication.
Kuschnig R., Ryabchikova T., Piskunov N.E., Weiss W.W., 1995, in *Stellar Surface Structure: Poster Proceedings*, proceedings of IAU Symposium 176, p. 135
Landstreet J.D., 1980, AJ 85, 611
Manset N. & Bastien P., 1995, PASP 107, 483

Mathys G., 1991, A&AS 89, 121
Michaud G. & Proffitt C.R., 1993, in *Peculiar Versus Normal Phenomena in A-Type and Related Stars*, ASP Conference Series, Vol. 44, p. 439
Press W.H. & Rybicki G.B., 1989, ApJ 338, 277
Preston G.W., 1967, ApJ 150, 547
Rice J.B., 1998, private communication
Rice J.B. & Wehlau W.H., 1994, PASP 106, 134
Schaller G., Schaerer D., Meynet G., Maeder A., 1992, A&AS 96, 269
Stepien K. & Dominiczak R., 1989, A&A 219, 197
Wade G.A., 1997, A&A 325, 1063
Wade G.A., Neagu E., Landstreet J.D., 1996a, A&A 307, 500
Wade G.A., Elkin V.G., Landstreet J.D., Leroy J.-L., Mathys G., Romanyuk I.I., 1996b, A&A 313, 209
Wade G.A., Bohlender D.A., Elkin V.G., Landstreet J.D., Romanyuk I.I., 1997a, A&A 320, 172
Wade G.A., Elkin V.G., Landstreet J.D., Romanyuk I.I., 1997b, MNRAS 292, 748
Wade G.A., Hill G.M., Manset N., Bastien P., 1997c, in *Stellar Magnetic Fields*, Special Astrophysical Observatory, Russian Academy of Sciences, p. 64
Wade G.A., Donati J.-F., Landstreet J.D., Mathys G., 1998, in preparation
Winzer J.E., 1974, Ph.D. Thesis, University of Toronto